

# Study of Raman Spectra of Nano-crystalline Diamond Like Carbon (DLC) films Composition ( $sp^2:sp^3$ ) with Substrate Temperature

Vikram S Yadav *Member IAENG*, Devendra K Sahu, Manveer Singh, Kuldeep Kumar

**Abstract**— Nano-crystalline Diamond like Carbon (DLC) film has been grown by Dense Plasma Focusing Method (DPF) using pure graphite Plasma, on different substrate (glass/silica) at different substrate temperature. The films were grown at substrate temperature  $100^{\circ}\text{C}$ ,  $150^{\circ}\text{C}$  &  $300^{\circ}\text{C}$  by the high dense plasma of energy 1.3 k Joule on glass and silica. Raman spectra confirmed that  $sp^3$  content in grown in the films under various conditions. The Raman spectra of these films show a broad asymmetric peak which narrow with decreasing  $sp^2$  contents. We believe that our data presented here may be used as reference of DLC characterization.

**Index Terms**— Raman Spectra, Substrate Temperature, DLC characterization etc.

## I. INTRODUCTION

Carbon is a versatile element that is found both allotropic forms in amorphous and crystalline state. Pure diamond ( $sp^3$ ) and graphite ( $sp^2$ ) are example of carbon state. Amorphous carbon is usually mixture of carbon atoms with  $sp^3$ ,  $sp^2$  and even  $sp^1$  bonding. An amorphous carbon with high fraction of diamond-like ( $sp^3$ ) bond is known as diamond like carbon (DLC). The term DLC was first used by Aisenberg and Chabot [1]. These films have aroused a considerable interest as coating material due to their attractive properties that are similar to diamond. DLC films can be deposited at low temperatures. Various methods have been developed for deposition of DLC films [2-10]. DLC films have a large number of applications such as wear-protective and antireflective coating for tri-biological tools, engine parts, razor blades and sunglasses, biomedical coatings and micro-electromechanical system. DLC films mainly consist of combination of four-fold

coordinated  $sp^3$  sites, as in diamond, and the three-fold coordinated  $sp^2$  sites, as in graphite. The deposition method

Manuscript received Monday, July 27, 2009.

**Vikram S Yadav, Ph.D.** is Reader in Applied Physics, with the Department of Applied Sciences, Bundelkhand Institute of Engineering and Technology, Jhansi, INDIA. 284128. (corresponding author to provide phone: +91-9415030412; fax: +91-510-2320349; e-mail: vikrams\_yadav@rediffmail.com).

**Devendra K Sahu, Ph.D.** is with Department of Basic Sciences, Bundelkhand University, Jhansi, INDIA. 284128. (e-mail: dkpolymer2003@yahoo.co.in).

**Manveer Singh** and **Kuldeep Kumar** are with Department of Physics & Electronics, S.G.T.B. Khalsa College, University of Delhi, New Delhi-110 007, INDIA

and growth condition determine the amount of  $sp^3$  and  $sp^2$  content in the film using Raman spectroscopy, as Raman spectroscopy is a non-destructive and fast for characterizing the carbon materials [11]. For visible excitation, Raman spectra for carbon show 'G' ( $1560\text{cm}^{-1}$ ), 'D' ( $1360\text{cm}^{-1}$ ), and for UV excitations 'T' ( $1060\text{cm}^{-1}$ ) peak in the  $800\text{-}2000\text{ cm}^{-1}$  region [12-16]. The G peak is due to the bond stretching of all pairs of  $sp^2$  atoms in both rings and chains. The D peak is due to the breathing modes of  $sp^2$  atoms in rings [17-20] The T peak is due to the C-C  $sp^3$  vibrations [15-17]. In the present paper we studied temperature dependent properties of Nano-crystalline DLC.

## II EXPERIMENTAL DETAILS

A DPF is the plasma machine that produces, short-lived plasma, which is so hot and dense that it becomes a copious multi-radiation source. A Mather type plasma focus device, energized by a  $9\ \mu\text{f}$ ,  $18\ \text{kV}$  discharged capacitor with used storage energy of  $1.3\ \text{kJ}$  was used coating Diamond like Carbon (DLC) on the silicon and quartz substrates. The schematic arrangement of the experimental setup along with the focus sub system is given in fig 2.1. The focus sub system is a coaxial electrode assembly with a tapered anode at the centre surrounded by a cathode comprising six equidistance systematic rods. The copper anode having an effective length of  $105\ \text{mm}$  is inserted with  $8\ \text{mm}$  deep pure graphite disc at the top. A high voltage power supply is used to charge the capacitor bank and a pressurized spark gap is used as a fast switching device for discharge the capacitor through electrodes inside the monitored using a high voltage focus chamber. The chamber is evacuated up to  $1 \times 10^{-3}$  mbar pressure by a rotary pump before admitting insert gas. The high probe is a simple resistance divider, with a response time of about  $15\ \text{ns}$  and is connected across the anode and cathode header. A high intensity spike in the voltage probe signal, as observed on the oscilloscope, indicate good focusing in this way an optimum value of working gas pressure is selected and is fixed for the rest of the experiment.

The substrates used in this experiment are quartz cut with dimensions of  $10 \times 10 \times 0.5\ \text{mm}$ . The substrates are mounted at different axial and angular position above the anode tip on a specially designed holder which is covered by the shutter. A set of three samples is placed at fixed axial position of  $8\ \text{cm}$  from the anode tip and varying angle of  $4^{\circ}$ ,  $8^{\circ}$  and  $12^{\circ}$  with respect to the anode axis. The shutter is used to avoid the substrate sample from week focus shots at the beginning of the experiment. Plasma focus operation is based on the pulsed

electrical discharged through gas contained between the co-axial electrode separated with a glass insulator sleeve. High voltage applied to the electrodes emerged in a low pressure gas causes an electrical breakdown along the insulator sleeve. First rise of the current leads to the formation of the plasma sheath. This is driven by self generated force, moves across the axis of electrodes towards the open end. After reaching the central electrode edge the sheath collapse toward the axis forming a dense ( $10^{20} \text{ cm}^{-3}$ ) and hot (1-2 kV) elongated plasma structure called "pinch". These abrupt changes induced high electric field which is associated with a magnetic field, drives the ions axial away from the central anode and electrons toward the anode to form ions and electron beams.

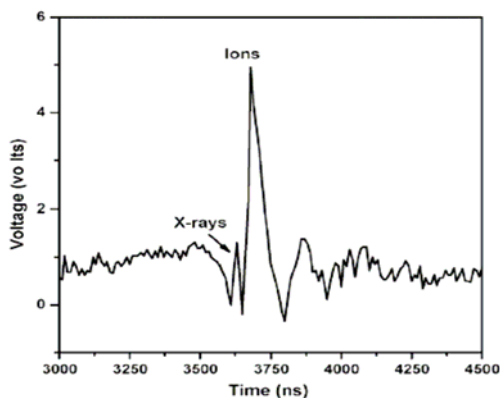


Fig 2.1:- Ion beam signal recorded by GaAs detector.

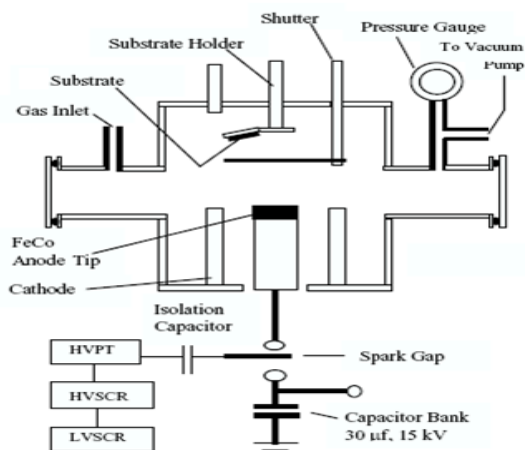


Fig 2.2 Diagram of DPF machine

The nitrogen ions emitted from the focus region basically obey  $dN/dE \sim E^k$  energy relation, where N is the number of ions having energy E and  $k \sim 3.5$  [21]. Number of ions is measured by using a photo conductive GaAs detector masked with a pin hole of 50 micro meter diameter, placed at the in front of target materials. It controls the numbers of ions passing through it. The operating voltage of the detector is 300 V and a Gould 4074A four channel digital storage oscilloscope records the signal. When the ion beam is incident on the detector, current is generated and the corresponding voltage is measured through oscilloscope fig-2.1.

### III RESULTS AND DISCUSSIONS

We have fabricated films at different substrate temperature other than room temperature, as 100°C, 150°C and 300°C and then characterize them by using X-Ray diffraction, SEM, AFM and Raman Spectroscopy techniques. Diffraction studies of the films were done using X-ray diffractometer (Philips PW 3020). The broader peaks were found. This is expected since DLC films are always found to be Nano- crystalline in nature. The particle size found around 60-80 nm.

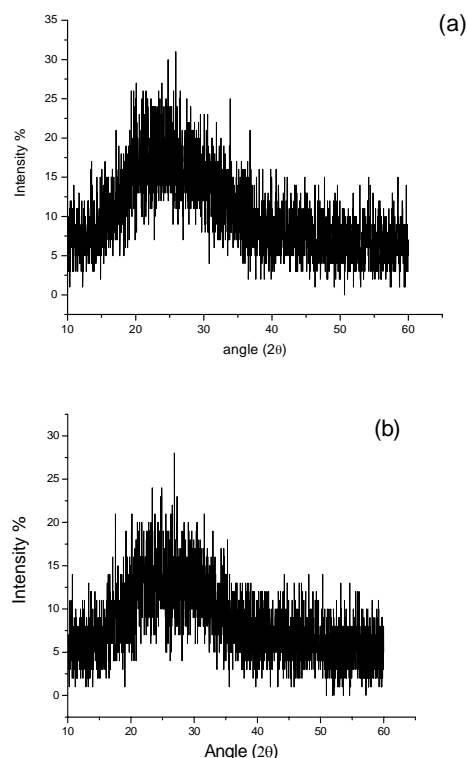


Fig 3.1:- Diffraction pattern of DLC films at (a) room temperature (b) 300°C temperature.

From the SEM micrograph of the DLC films, the grown graphite films texture can be observed. However, the Nano-crystalline nature of film grown on substrates kept at higher temperature is evident from fig 3.2(b).

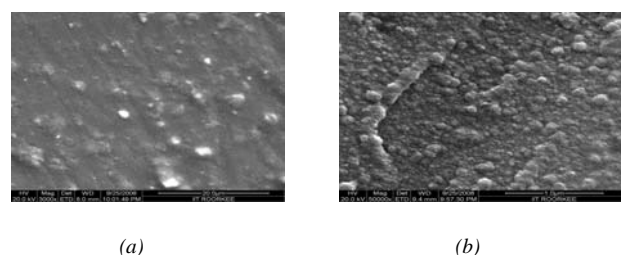
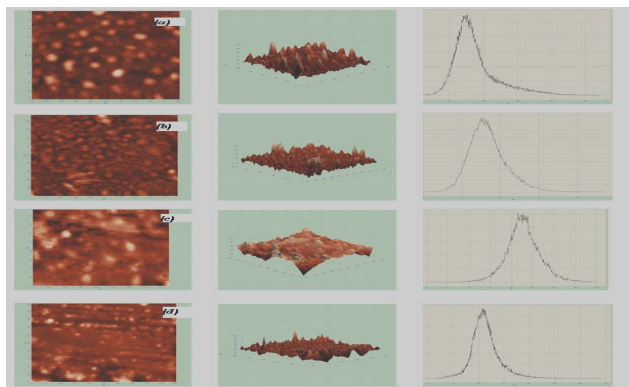


FIG3.2:- SEM micrograph of the films grown at (a) room temperature and (b) 300°C.

However, for completeness of our investigation of film surface, we have also studied the surface using Atomic Force Microscope (AFM), Fig3.3. The figure shows the film surface to be smooth with surface roughness to be of the order 10-20 nm and Particles size calculated AFM micrograph is 60-08 nm.



**Fig 3.3:- AFM micrograph of the films grown at (a) Room temperature, (b) 100°C, (c) 150°C and (d) 300°C.**

Raman spectroscopy is the powerful tool to determine the relative content of the  $sp^2$  and  $sp^3$  bonding in the film. The Raman spectroscopy in this work tells us about the quality of the deposited thin films by DPF method. As can be seen from fig 3.4, the Raman spectra of our films show two overlapping peaks. These peaks are the 'G' and 'D' peaks associated with  $sp^2$  bonding in graphite. The fraction of  $sp^3$  bonding present in the film can be evaluated by the peak position of the 'G' peaks. Also, rich information for confirming the formation of  $sp^3$  bonds can be obtained from the area, Full Width Half Maxima (FWHM) and relative intensity of 'D' and 'G' peaks. However, since these peaks overlap, we have to de-convolute them. The simplest function employed de-convolute is two Lorentzians or two Gaussians. Raman spectra of DLC films at different temperature tell about the  $sp^2$  and  $sp^3$  bonding present in the thin film state.

The disordered, amorphous and carbon phase in Nano-crystalline DLC films can be characterized by measuring the position and width of G-peak and intensity ratio of G-and D-peaks in Raman spectra, rather than by directly measuring their intensities. The changes in line shape of the Raman spectrum for carbon material, when its phase changes from graphite to non-crystalline carbon (stage one) to amorphous carbon (stage two) and then to ta-C with about 85-90%  $sp^3$  bonding (stage three), have been explicitly shown in their article. During the first stage, with an increase in  $sp^3$  contents in the materials, the ratio of the intensity of 'D' peak ( $I_D$ ) to that of 'G' peak ( $I_G$ ) increases from 0.0 to 0.2 and simultaneously, the 'G' peak position ( $\omega_G$ ) increase from 1580  $cm^{-1}$  to 1600  $cm^{-1}$ . However, in the second stage, a reverse trend is observed for both parameters with increases in  $sp^3$  contents: the ratio  $I_D/I_G$  decreases from 2.0 to 0.25, whereas, the value of  $\omega_G$  decreases from 1600 to 1510  $cm^{-1}$ . The  $sp^3$  contents can be calculated using this relation.

$$Sp^3 \text{ contents} = 0.24 - 48.9(\omega_G - 0.1580)$$

In this equation,  $\omega_G$  has been taken in unit of inverse of micrometer unit. In addition to  $\omega_G$ , the intensity ratio of the D- and G peaks can also be used to estimate the above parameters of DLC films. This method is not fruitful, reasons being that the intensity of the D peak is quite low compared to that of G peak in our samples and at low frequency, Raman spectra the weak D-peak coexists with Raman components of other phases of carbon; hence the measured intensity of the D-peak from the curve fitting is not unique, it varies strongly with the choice of width and intensity of other nearby peaks.

The D-peak present at the wave number 1340 $cm^{-1}$  and G-peak at the wave number 1595  $cm^{-1}$ , which implies DLC Intensity ratio found 78.82% at 0°C temperature. The D-peak present at the wave number 1358 $cm^{-1}$  and G-peak at 1580  $cm^{-1}$ , which implies DLC Intensity ratio found 87.04% at 300°C. The measured intensity of the D-peak from the curve fitting is not unique, it varies strongly with the choice of width and intensity of other nearby peaks. The D-peak present at the wave number 1340 $cm^{-1}$  and G-peak at the wave number 1595  $cm^{-1}$ , which implies DLC Intensity ratio found 78.82% at 0°C temperature. The D-peak present at the wave number 1358 $cm^{-1}$  and G-peak at 1580  $cm^{-1}$ , which implies DLC Intensity ratio found 87.04% at 300°C.

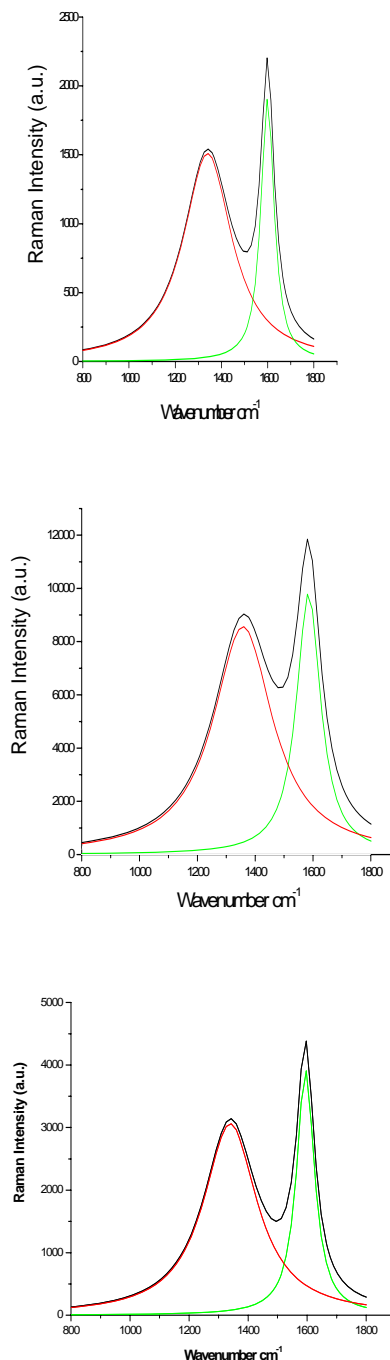


**Fig 3.4:- Fitting of D and G bands in Raman spectra of DLC films at (a) 100°C (b) 150°C (c) 300°C**

**Table 1:  $sp^3$  contents at different temperature**

Temp. °C	I (D)	I (G)	FWH M	Position of G peak	Sp <sup>3</sup> contents	I (D) / I (G)
100	1504	1912	68.7	1597	0.157	78.66
150	3056	3900	200	1594	0.171	77.25
300	8534	9776	100.8	1584	0.220	87.30

The variation of  $sp^3$  contents with temperature shows a linear relation as shown in fig 3.5. This indicates that at higher substrate temperature,  $sp^3$  contents will be higher.

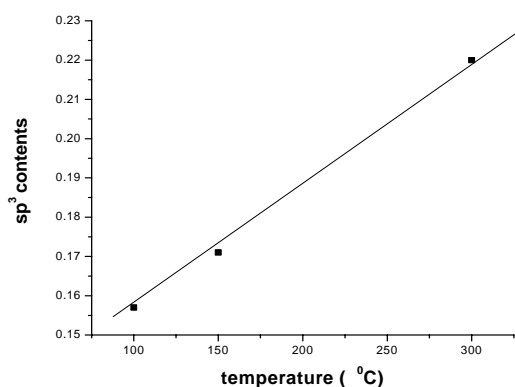


**Fig.**

### 3.5 Variation of $sp^3$ contents with temperature.

#### IV CONCLUSION

The deposited films are of amorphous (Nano-crystalline) in nature, shown by the X-Ray pattern, which is conforms by the grain present in the AFM. The order of the grains is of the nanometer (60-80 nm). The Raman spectra explain the ratio of the bonding  $sp^2$  and  $sp^3$  as found to be increasing function of substrate temperature. Before this work, the deposition on quartz is reported rarer. Deposition of DLC thin films at quartz by Dense Plasma Focusing (DPF) gives better results with the heated substrate and shows linear relationship. The tribological applications of DLC films explain their resistant properties.

#### REFERENCES

[1] S. Aisenberg and R.Chabot, *J.Appl.Phys.*, 42, 2953 (1971).  
 [2] A.G.Fitzgerald, M.Simpson, G.A.Dederski, P.A.Moir, A.Matthews and D.Tither, *Carbon*, 26, 229 (1988).  
 [3] J.Ullman, G.Schmidt and W.Schra, *Thin Solid Films* 214, 35 (1992).  
 [4] E.Eldrige, G.A.Clarke, Y.Xie and R.R.Parsons, *Thin Solid Films* 280, 13 (1996).

[5] N.H.Cho, K.M.Krishnan, D.K.Veirs, M.D.Rubin, C.B.Hooper, B.Bunsha and D.B.Bogy, *J.Mater.Res.*5, 2543(1990)  
 [6] C.Weissmantel, C.Schurer, F.Frolich, P.Grau and H.Lehman, *Thin Solid Films* 61, L5 (1979).  
 [7] J.J.Cuomo, J.P.Doyle, J.Bruley and J.C.Liu, *J.Vac.Sci.Technol.* A9, 2210(1991).  
 [8] J.Smith, A. Dehbi and A.Matthews, *Relat. Mater.* 1,355 (1992).  
 [9] F.Akatsuka, Y.Hirose and K.Komaki, *Jpn. J. Appl. Phys.*, 27, L1(1988).  
 [10] J.Koskinen, *J.Appl.Phys.* 63, 2094 (1988).  
 [11] A. C. Ferrari and J. Robertson, *Philos. Trans. R. Soc. London, Ser. A* **362**, 2267 (2004).  
 [12] A. C. Ferrari and J. Robertson, *Phys. Rev. B* **61**, 14095 (2000).  
 [13] A. C. Ferrari and J. Robertson, *Phys. Rev. B* **64**, 075414 (2001).  
 [14] S. Piscanec, F. Mauri, A. C. Ferrari, M. Lazzeri, and J. Robertson, *Diamond Relat. Mater.* **14**, 1078 (2005).  
 [15] K. W. R. Gilkes, S. Praver, K. W. Nugent, J. Robertson, H. S Sands, Y. Lifshitz, and X. Shi, *J. Appl. Phys.* **87**, 7283 (2000).  
 [16] V. I. Merkulov, J. S. Lannin, C. H. Munro, S. A. Asher, V. S. Veerasamy, and W. I. Milne, *Phys. Rev. Lett.* **78**, 4869 (1997).  
 [17] F. Tuinstra and J. L. Koenig, *J. Chem. Phys.* **53**, 1126 (1970).  
 [18] C. Castiglioni, E. Di Donato, M. Tommasini, F. Negri, and G. Zerbi, *Synth. Met.* **139**, 885(2003).  
 [19] S. Piscanec, M. Lazzeri, F. Mauri, A. C. Ferrari, and J. Robertson. *Phys. Rev. Lett.* **93**, 185 (2004).  
 [20] C. Mapelli, C. Castiglioni, G. Zerbi, and K. Mullen, *Phys. Rev. B* **60**, 12710 (2000).  
 [21] W. Stygar. G. Gerdin. F. Vennri. J. Mandrekas. *Nuel. Fusion* 22(1982). 2543 (1990).